URSI GASS 2021, Rome, Italy, 28 August - 4 September 2021

Radio Frequency Interference Mitigation Method for Synthetic Aperture Radar Using Joint Low Rank and Sparsity Property

Yi Ding, Jinbiao Du, Zhaodong Zhang, Weiwei Fan, Feng Zhou*
Key Laboratory of electronic information countermeasure and simulation technology of ministry of education, Xidian University, 710071 Xi'an, China

Abstract

Radio frequency interference (RFI) is a severe issue for synthetic aperture radar (SAR), which is unavoidable for complex electromagnetic environment and the large imaging band. The presence of RFI would reduce the signal-to-noise ratio (SNR) and influence the image interpretation. This paper proposes a RFI mitigation method joint the low rank and double sparsity (LRDS-IM) characteristics in time-frequency (TF) domain. On the basis of TF analysis, we introduce the low rank and sparse characteristics to establish a precise RFI reconstruction model. In virtue of the alternate direction iteration strategy, we can separate the SAR echo into the RFI matrix and target signal matrix. Meanwhile, the well-focused SAR image is obtained cooperating with the state-of-the-art imaging algorithm. Finally, the RFI mitigation experiments of the measured SAR data verify the effectiveness of the proposed algorithm.

1 Introduction

Thanks for the characteristics of all-day, all-weather, high resolution, and long-range, SAR has been applied in various fields. However, SAR is inevitable to be polluted by RFI, as for the numerous electromagnetic equipment and large imaging band. The presence of RFI would reduce SNR of the echo and prevent the accurate imaging parameters estimation, resulting in blurry and defocused SAR images. Moreover, it would pose a hindrance for target inversion and image interpretation [1-2]. Therefore, it is urgent to study the advanced RFI mitigation algorithms to decrease the negative effects of RFI.

Generally, RFI can be divided into narrow-band interference (NBI) and wide-band interference (WBI) according to the bandwidth ratio of interference to the target echo (usually set as 1%). For the pursuit of better SAR images, multitudinous algorithms were proposed to handle RFI in different data domain over the past decades. In frequency domain, notch filtering [3] and maximum a posterior estimation [4] methods are introduced by the assumption that NBI concentrated on the limited frequency points. In time domain, the subspace projection methods [5-6] based on principle component analysis and independent component analysis are proposed. However, these algorithms only utilize the partial characteristics of spectrum or temporal, which is insufficient for signal separation with RFI sometimes. Therefore, the researchers introduce the mitigation algorithms joint time and frequency information via time-frequency analysis technology [7-8]. Su *et al.* use the robust principle component analysis method to achieve mitigation in TF domain, which is based on the low rank assumption for RFI and sparse hypothesis for target echo. It utilizes the structure characteristics to separate RFI and target echo in observed data, but the precision of interference reconstructed can be promoted further.

In this paper, we propose a RFI mitigation scheme joint the low rank and double sparsity (LRDS-IM) characteristics in TF domain. Firstly, we utilize short-time Fourier transform (STFT) to represent the echoes in the TF domain. Meanwhile, we formulate a signal separation model for the low rank and sparse RFI with sparse target echo. Then, an alternative direction iteration strategy is introduced to estimate the different components. At last, the mitigation results of airborne and spaceborne SAR measured data verify the effeteness of LRDS-IM algorithm.

2. Theory and Methodology

2.1 Signal Modeling

The received SAR echo can be expressed as a linear superposition of original target echo, interference and additive noise.

$$x(k) = i(k) + s(k) + n(k) \tag{1}$$

where k represents the distance snapshot, and x , i , s , n denote the received SAR echo, RFI, target echo and additive noise, respectively. In order to explore the characteristics of the echo, STFT is utilized to represent it into the range TF domain.

$$\mathbf{STFT_X} = \mathbf{STFT_I} + \mathbf{STFT_S} + \mathbf{STFT_N} \tag{2}$$

Where $\mathbf{STFT_X}$, $\mathbf{STFT_I}$, $\mathbf{STFT_S}$ and $\mathbf{STFT_N}$ denote the TF matrixes of the received echo, RFI, target echo and noise, respectively. In a way, RFI mitigation is equivalent with a separation problem for RFI and target echo, thus we can formulate an optimization criterion further based on minimizing reconstruction error:

$$\min_{\mathbf{STFT_I},\mathbf{STFT_S}} f\left(\mathbf{STFT_X}, \mathbf{STFT_I}, \mathbf{STFT_S}\right) \tag{3}$$

2.2 low rank and sparsity

As for the RFI includes NBI and WBI, we analysis the characteristics of RFI in measured data respectively. Fig. 1(a) and (d) are the TF spectrograms of two azimuth echoes contaminated NBI and WBI respectively. Since the higher amplitude of RFI, the bright areas in the TF spectrum mean the RFI, which only occupies a limited part. And we perform eigenvalue decomposition on the TF matrix to obtain its eigenvalue distribution. Fig. 1(b) and (e) are the eigenvalue distribution of the TF spectrograms. The results show that large eigenvalues corresponding to RFI are in the minority, indicating a low-rank structure.

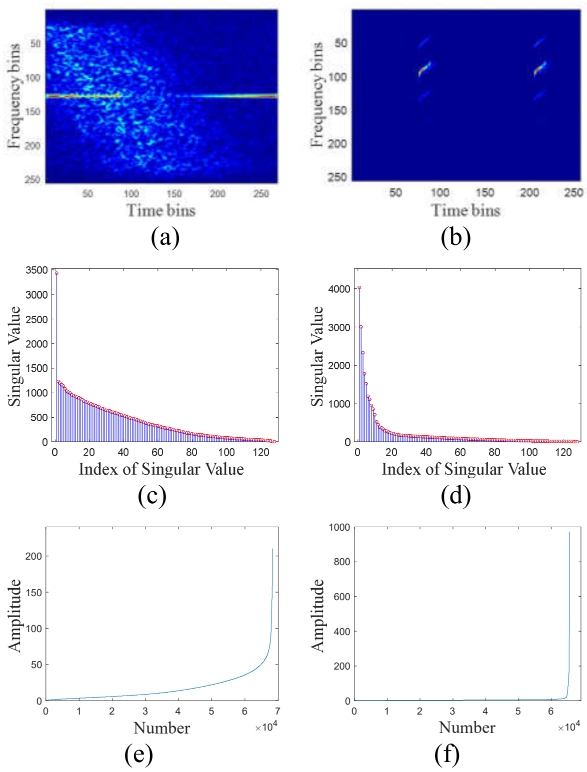

Fig. 1 TF spectrum analysis of RFI. (a) TF spectrum, (c) eigenvalue distribution and (e) amplitude distribution are for NBI. (b) TF spectrum, (d) eigenvalue distribution and (f) amplitude distribution are for WBI.

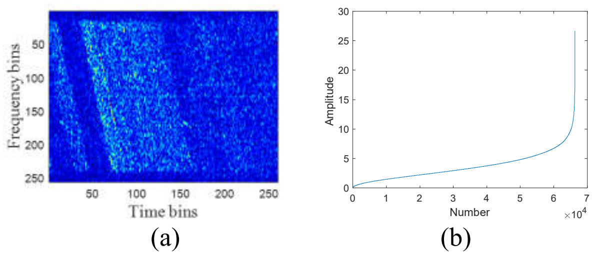

Fig. 2 TF spectrum analysis of the measured echo without RFI. (a) TF spectrum. (b) Amplitude distribution.

Meanwhile we further analyze the amplitude distribution of the echo with and without RFI, which are shown in Fig. 1(c), (f) and Fig. 2 (b). They indicate that RFI and target echo are sparsely distributed at different degrees in TF domain respectively. Therefore, the RFI matrix can be treated as a low rank and sparse matrix, while a sparse matrix for target echo.

2.3 RFI Mitigation Methodology

Without loss of generality, we can assume that the observed noise obeys the complex Gaussian distribution corresponding to the L_2 norm, and the optimization function is rewritten as:

$$\min_{\mathbf{STFT_I},\mathbf{STFT_S}} \left\|\mathbf{STFT_X}-\mathbf{STFT_I}-\mathbf{STFT_S}\right\|_F^2 \tag{4}$$

Where $\|\bullet\|_F^2$ represents the Frobenius norm. Based on the foregoing analysis, the observation matrix $\mathbf{STFT_X}$ can be decomposed into two independent components: low rank and sparse RFI matrix as well as sparse target echo matrix. The optimization problem can be specified as:

$$\begin{cases} \min\limits_{\mathbf{STFT_I},\mathbf{STFT_S}} \left\|\mathbf{STFT_X}-\mathbf{STFT_I}-\mathbf{STFT_S}\right\|_F^2 \\ \quad s.t.\ \ \mathrm{rank}\left(\mathbf{STFT_I}\right)\le r \\ \quad\quad\ \ \mathrm{card}\left(\mathbf{STFT_I}\right)\le k_1 \\ \quad\quad\ \ \mathrm{card}\left(\mathbf{STFT_S}\right)\le k_2 \end{cases} \tag{5}$$

Where $\mathrm{rank}(\bullet)$ and $\mathrm{card}(\bullet)$ denote the rank operator and cardinality. r represents the rank of $\mathbf{STFT_I}$, k_1 ,k_2 represent the sparsity degrees of $\mathbf{STFT_I}$ and $\mathbf{STFT_S}$. In order to separate the RFI with target echo by managing the optimization problem in (5), it can be divided into two subproblems and tackled alternatively until convergence.

$$\begin{cases} \mathbf{STFT_I}^{(t+1)} = \mathop{\arg\min}\limits_{\substack{\mathrm{rank}(\mathbf{STFT_I})\le r \\ \mathrm{card}(\mathbf{STFT_I})\le k_1}} \left\|\mathbf{STFT_X}-\mathbf{STFT_I}-\mathbf{STFT_S}^{(t)}\right\|_F^2 \\ \mathbf{STFT_S}^{(t+1)} = \mathop{\arg\min}\limits_{\mathrm{card}(\mathbf{STFT_S})\le k_2} \left\|\mathbf{STFT_X}-\mathbf{STFT_I}^{(t+1)}-\mathbf{STFT_S}\right\|_F^2 \end{cases} \tag{6}$$

After the several alternate iterations, we can get the separation result of RFI and recover target echo through cancellation in the TF domain. The specific mathematical expression is

$$\hat{x}(k) = ISTFT\left[\mathbf{STFT_X}-\mathbf{STFT_I^*}\right] \tag{7}$$

Where $ISTFT[\bullet]$ is the inverse STFT operator. The RFI mitigation algorithm for single pulse is given above, and we can process pulse by pulse to obtain the RFI-free SAR data. Incorporating with the state-of-the-art imaging algorithms, a SAR imaging result without RFI can be obtained.

3 Experimental Results

In this section, the effectiveness of the proposed RFI mitigation algorithm is verified based on the measured RFI-corrupted SAR data. Meanwhile, we compare the RFI mitigation performance with the go decomposition

(GoDec) algorithm [8], that the experimental results further demonstrate the superiority. Moreover, qualitative and quantitative metrics are utilized to evaluate the performance of different algorithms.

3.1 Result of measured data with NBI

Firstly, the mitigation experiments are performed on the measured data with NBI, which was recorded by X-band airborne SAR. Fig. 3 (a) presents the original imaging result without applying RFI suppression, where the bright lines overshadow the buildings and fields. Fig. 3(b) shows the SAR image after GoDec process. Although the majority of the NBI has been mitigated, the image is defocused in places because of signal loss, which is an obstacle for precise image interpretation. Fig. 3(c) presents the SAR image applying the proposed algorithm. It is obviously that the image is well focused and the NBI has been suppressed effectively, facilitating the target discrimination. To evaluate the performance of the proposed algorithm, we introduce two metrics in image domain to further discuss.

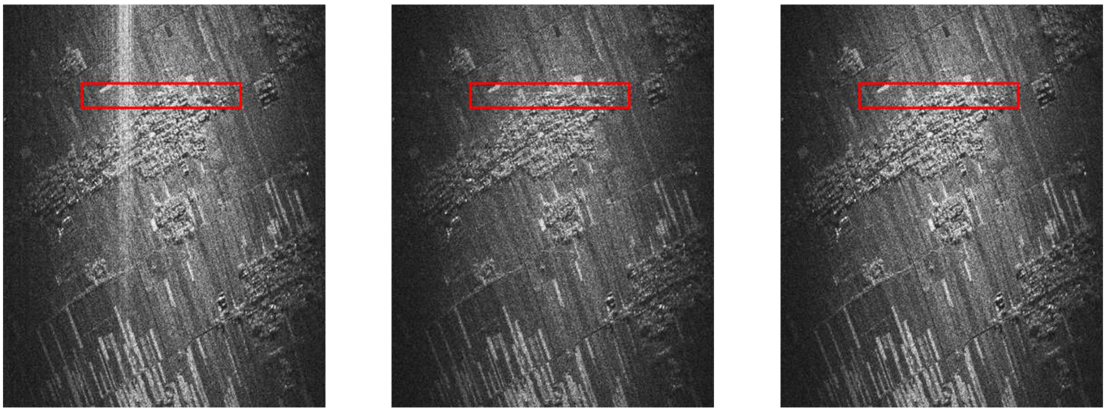

Fig. 3 Mitigation results. (a)The SAR image without interference mitigation. (b) The SAR image after applying the GoDec algorithm. (c) The SAR image after applying the LRDS-IM algorithm.

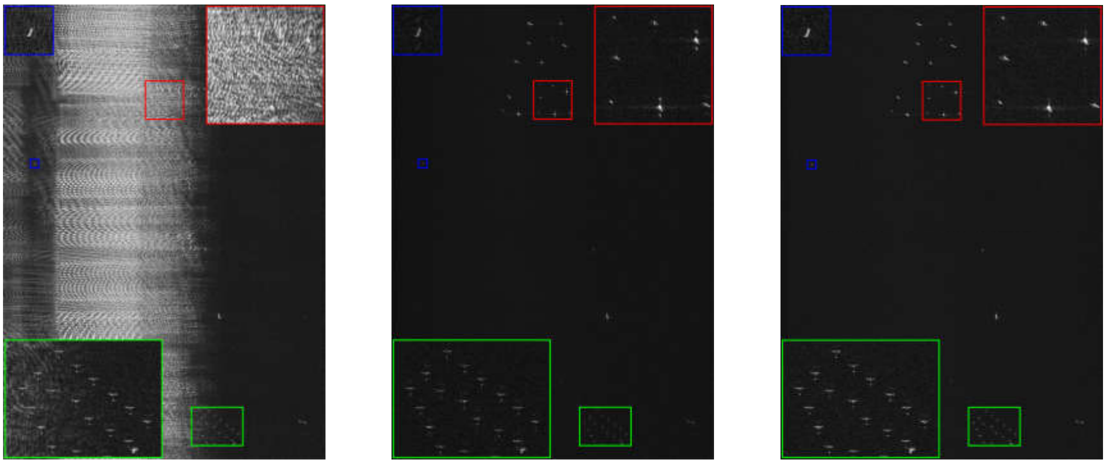

Fig. 4 Mitigation results. (a)The SAR image without interference mitigation. (b) The SAR image after applying the GoDec algorithm. (c) The SAR image after applying the LRDS-IM algorithm.

Table I SAR image quality evaluation

Metrics / Method	AG(dB)	GLD(dB)
GoDec	10.765	87.006
LRDS-IM	11.204	93.920

Average gradient (AG) represents the sharpness of image, and the abundance of image details, expressed as:

$$AG = \frac{\sum_{m=1}^{M}\sum_{n=1}^{N}\sqrt{\left(\partial I(m,n)/\partial m\right)^2 + \left(\partial I(m,n)/\partial n\right)^2}}{4(M-1)(N-1)} \quad (8)$$

Where $\partial I(m,n)/\partial m$ and $\partial I(m,n)/\partial n$ respectively denotes the vertical and horizontal gradients of the image. The larger the AG value, the clearer the edge features of the SAR image.

Gray level difference (GLD) can measure the gray level change of SAR image. The specific mathematical representation is:

$$GLD = \frac{\sum_{m=1}^{M}\sum_{n=1}^{N}\left(\left|I(m,n)-I(m+1,n)\right|+\left|I(m,n)-I(m,n+1)\right|\right)}{(M-1)(N-1)} \quad (9)$$

A lager GLD is better for the image. The two metrics listed in Table I indicate that the proposed algorithm have better performance and more details comparing to GoDec algorithm.

3.2 Result of measured data with WBI

To further demonstrate the effeteness of LRDS-IM on WBI-contaminated data, we performed mitigation experiments for another measure data recorded by C-band Sentinel-1 satellites of the European Space Agency (ESA). The mitigation results shown in Fig. 4. Fig. 4 (a) represents the SAR imaging result without interference mitigation, in which ships are covered by WBI. Fig. 4 (b) and (c) shows the SAR imaging results after applying GoDec and the proposed algorithm. From the reconstruction results in the SAR image, it can be seen that the RFI has been mitigated thoroughly both in GoDec and LRDS-IM results. However, the ship targets are defocused and on a low side due to the signal loss in the GoDec result, while they are well-focused after applying the LRDS-IM algorithm. In addition, the evaluation metrics are performed as Table II, which supports the fact that LRDS-IM has more abundant details.

Table II SAR image quality evaluation

Method \ Metrics	AG(dB)	GLD(dB)
GoDec	2.206	17.997
LRDS-IM	2.617	21.283

4. Conclusion

In this paper, a LRDS-IM algorithm in TF domain is introduced for SAR data. It takes advantages of the signal separation technology that the observation TF matrix can be separated as the superposition of joint low rank and sparse RFI matrix, sparse target echo matrix and noise matrix. Based on TF analysis, we employ the low rank and sparse characteristics to formulate a precise RFI reconstruction model. And we tackle the optimization problem through the alternate direction iteration strategy. Meanwhile, the effectiveness and superiority of the proposed algorithm was verified based on two measured data acquired by the airborne and sapceborne SAR. Also, the AG and GLD are adopted to evaluate the performance of RFI mitigation performance, which further demonstrate effectiveness of LRDS-IM algorithm.

5. Acknowledgements

Thanks to all the anonymous reviewers and editors for their comments and suggestions to this article, so that the content of this article can be more rigorous and plentiful. Meanwhile, the authors are grateful for the open-source sentinel-1 satellite SAR data of ESA, which has effectively supported the verification of the algorithm in this paper. This work was in part by National Natural Science Foundation of China under grant 61801344, 61801347, 61631019, 62001350, China Postdoctoral Science Foundation under grant 2016M602775, 2017M613076, 2020M673346, the Postdoctoral Science Research Projects of Shaanxi Province, and Natural Science Basic Research Plan in Shaanxi Province of China (Program No. 2020JQ-312). It was also supported by the Aeronautical Science Foundation of China under grant 20180181003, the Young Scientist Award of Shaanxi Province under grant 2015KJXX-19, 2016KJXX-82, the Joint Fund of Ministry of Education under grant 6141A02022367, and the Fundamental Research Funds for the Central-University under grant XJS200204, and with the Innovation Fund of Xidian University.

6. References

1. M Tao, J Su, Y Huang, L Wang, "Mitigation of Radio Frequency Interference in Synthetic Aperture Radar Data: Current Status and Future Trends," MDPI Remote. Sens.11,20, Oct. 2019, pp.2438. doi:10.3390/rs11202438.

2. P. De Matthaeis, R. Oliva, Y. Soldo, "Spectrum management and its importance for microwave remote sensing," IEEE Geosci. Remote Sens. Mag., 2018, 6, 17–25. doi:10.1109/MGRS.2018.2832057.

3. R. T. Lord, "Radio frequency interference suppression applied to synthetic aperture radar data," in Gen. Assem. Int. Union Radio Science, URSI GASS, 2005.

4. Y. Guo, F. Zhou, M. Tao, and M. Sheng, "A new method for SAR radio frequency interference mitigation based on maximum a posterior estimation," in Gen. Assem. Int. Union Radio Science, URSI GASS, Montreal, QC, Canada, Aug. 2017. pp. 1–4. doi:10.23919/ URSI GASS. 2017.8104495.

5. F. Zhou, R. Wu, M. Xing, and Z. Bao, "Eigensubspace-based filtering with application in narrow-band interference suppression for SAR," IEEE Geosci. Remote Sens. Lett., vol. 4, no. 1, pp. 75–79, Jan. 2007. doi:10.1109/ LGRS. 2006.887033.

6. M. Tao, F. Zhou, J. Liu, Y. Liu, et al., "Narrow-Band Interference Mitigation for SAR Using Independent Subspace Analysis," IEEE Trans. Geosci. Remote Sens., vol. 52, no. 9, pp. 5289–5301, Sep. 2014. doi:10.1109/ TGRS. 2013.2287900.

7. W Fan, F Zhou, M Tao, X Bai, P Rong, S Yang, T Tian. "Interference Mitigation for Synthetic Aperture Radar Based on Deep Residual Network," MDPI Remote. Sens. 11,14, Jul. 2019, pp.1654. doi:10.3390/rs11141654.

8. J Su, H Tao, M Tao, L Wang, J Xie, "Narrow-band interference suppression via RPCA-based signal separation in time-frequency domain," IEEE J. Sel. Topics Appl. Earth Obs. Remote Sens. 10,11, Aug. 2017, pp.5016–5025. doi:10.1109/ JSTARS.2017.2727520.